Excitation of Quadrupole and Octupole Levels of ^{12}C, ^{16}O, and ^{40}Ca by 156-MeV Protons*

R. M. HAYBRON†
Oak Ridge National Laboratory, Oak Ridge, Tennessee
and
Michigan State University, East Lansing, Michigan

AND

H. MCMANUS‡
Michigan State University, East Lansing, Michigan

(Received 3 June 1965)

The inelastic cross sections and polarizations for the excitation of some observed 2^+ and 3^- levels of ^{12}C, ^{16}O, and ^{40}Ca by 156-MeV protons were calculated in the distorted-wave, impulse approximation using the particle-hole transition densities of Gillet and collaborators. The results were compared with available experimental data and good qualitative agreement was obtained; in particular the particle-hole densities provided the necessary enhancements of the cross sections. Fits were also attempted using the theory of collective excitations. These provide reasonable fits to the cross-section data, but not to the polarization.

I. INTRODUCTION

THE particle-hole wave functions obtained by Gillet and Vinh-Mau[1] (GVM) for ^{12}C and ^{16}O and Gillet and Sanderson[2] (GS) for ^{40}Ca provide transition densities which are in generally good agreement with inelastic-electron-scattering data.[3] These wave functions can also be used in the analysis of high-energy proton-scattering data. The development of the high-energy, distorted-wave, impulse approximation (DWIA)[4] and the existence of fast computer codes suitable to the purpose[5] makes such an analysis possible.

Calculations were performed for the excitation of the 4.4-MeV, 2^+ and 9.6-MeV, 3^- levels of ^{12}C; the 6.13-MeV, 3^- and 15.3-MeV, 3^- levels of ^{16}O; and the 3.7-MeV, 3^- and 6.8-MeV, 3^- levels of ^{40}Ca. The results will be compared with experiment in Sec. IV. In Sec. II we describe briefly the use of the particle-hole wave functions in the DWIA. Section III contains a description of the DWIA calculations. The portion of the two-nucleon amplitude which is effective in exciting these levels is discussed in Sec. VIII. Finally in Sec. IX the results obtained using the collective picture for the excitations are presented.

II. TRANSITION AMPLITUDE

The distorted-wave impulse approximation (DWIA) form of the inelastic transition amplitude which corresponds to the notation in Ref. 5 is

$$T_{fi}=\frac{2\sqrt{2}h^2}{(2\pi)^3 m_p}\sum_{lss'\lambda\lambda'} d_{\lambda\lambda'}{}^{SS'}(E_0,\theta)C(lS'J_f\colon M_f-\lambda',\lambda')\times\sum_{n_a n_b}\langle\tfrac{1}{2}||\sigma^s||\tfrac{1}{2}\rangle C(\tfrac{1}{2}S\tfrac{1}{2}\colon n_a\lambda n_b)\times\int\chi_{m_b n_b}{}^{(-)*}(\mathbf{r})Y_e{}^{M_f-\lambda'*}\times F^{lS'J}(r)\chi_{n_a m_a}{}^{(+)}(\mathbf{r})d\mathbf{r}. \quad (1)$$

The amplitude describes the inelastic scattering of a proton of energy E_0 in a spin state m_a to a spin state m_b accompanied by the excitation of an even-even nucleus from a 0^+, $T=0$ ground state to an excited state J_f, M_f, T_f ($T_f=0$ or 1). The quantities $\chi^{(+)}$ and $\chi^{(-)}$ are the distorted waves describing the motion of the proton before and after the inelastic event, respectively. The proton-spin subscripts on the χ's indicate that these functions are matrices in the spin space of the scattered particle due to spin-orbit coupling in the optical potential. S is the spin transfer to the *scattered* proton: S' is a similar quantity for the target nucleon. For normal parity transitions, the orbital angular momentum transfer to the nucleus $l=J_f$ and $S'=0$ or 1. For spin-flip transitions, (abnormal parity case), $S'=1$ and $l=J_f-1$ and J_f+1. The quantity $d_{\lambda\lambda'}{}^{SS'}(E_0,\theta)$ contains all the information about the nucleon-nucleon interaction and is a function of the incident energy as well as the nucleon-nucleus scattering angle θ in the approximation adopted here (see Ref. 5); m_p is the proton rest mass.

The transition density $F^{lS'J}(r)$ is defined as

$$F^{lS'J}(r)=\sum_\nu\frac{(2j_B+1)^{1/2}}{(2J_f+1)^{1/2}}\times\langle j_B(l_B,\tfrac{1}{2})||\mathcal{Y}_{J_f}(l,S')||j_A(l_A,\tfrac{1}{2})\rangle\times u_{n_B l_B}{}^*(r)u_{n_A l_A}(r)\alpha_\nu. \quad (2)$$

* Research sponsored by the U. S. Atomic Energy Commission under contract with the Union Carbide Corporation and Michigan State University.

† On loan to Oak Ridge National Laboratory from Michigan State University.

‡ Guggenheim Foundation and Nordita Fellow, 1963–64.

[1] V. Gillet and N. Vinh Mau, Nucl. Phys. **54**, 321 (1964).
[2] V. Gillet and E. A. Sanderson, Nucl. Phys. **54**, 472 (1964).
[3] V. Gillet and M. A. Melkanoff, Phys. Rev. **133**, B1190 (1964).
[4] A. K. Kerman, H. McManus, and R. M. Thaler, Ann. Phys. (N. Y.) **8**, 551 (1959).
[5] R. M. Haybron and H. McManus, Phys. Rev. **136**, B1730 (1964).

TABLE I. The coefficients defined in Eq. (3) for the levels of ^{12}C. The 2^+ state is found experimentally at 4.43-MeV and the 3^- state at 9.6 MeV. The labeling of the hole-particle pairs is: hole state above, particle state below. The coefficients for the levels of ^{16}O and ^{40}Ca may be obtained from Refs. 1 and 2 using Eq. (3).

	$1p_{3/2}$ $1p_{1/2}$	$1p_{3/2}$ $1f_{5/2}$	$1p_{3/2}$ $1f_{7/2}$	$1p_{3/2}$ $2p_{1/2}$	$1p_{3/2}$ $2p_{3/2}$	$1p_{1/2}$ $1d_{3/2}$	$1s_{1/2}$ $1d_{5/2}$
(I) 2^+, $T=0$: 8.23 MeV	0.94	−0.05	0.23	0.07	−0.07	−0.13	0.19
(II) 2^+, $T=0$: 4.80 MeV	0.96	−0.02	0.32	0.19	−0.21	−0.34	0.49
	$1p_{3/2}$ $1d_{3/2}$	$1p_{3/2}$ $1d_{5/2}$					
(I) 3^-, $T=0$: 13.4 MeV	−0.47	0.88					
(II) 3^-, $T=0$: 12.8 MeV	−0.61	0.99					

(The notation $\langle|| \; ||\rangle$ denotes reduced matrix element as defined in Brink and Satchler.[6]) This function is a sum of particle-hole contributions where the hole has quantum numbers n_A, j_A, l_A and the particle n_B, j_B, l_B. The radial wave functions $u_{n_Al_A}$ and $u_{n_Bl_B}$ are oscillator functions. $\mathcal{Y}_{J_f}$ is a spherical tensor operator of rank J_f in the spin-angle space of the target nucleon obtained by coupling Y_l and $\sigma^{S'}$. The coefficients α_ν are obtained from structure calculations. Here we shall use

$$\alpha_\nu = (-1)^{j_A+\frac{1}{2}}(X_\nu + Y_\nu) , \qquad (3)$$

where X_ν and Y_ν (Ref. 1) are the particle-hole amplitudes for particle-hole pair ν from forward and backward-going graphs, respectively. The Y_ν then represents approximately the effect of ground-state correlations in the random-phase approximation (RPA). The phase factor in (3) is necessary to make the calculation of the transition amplitude in Ref. 4 consistent with the phase convention employed in obtaining the X's and Y's.[7]

III. CALCULATIONS

The transition amplitude in Eq. (1) was used to compute the inelastic cross sections and some polarizations for the levels of ^{12}C in Table I and those of ^{16}O and ^{40}Ca mentioned before. The calculations were done using both the approximation I and approximation II transition densities (hereafter referred to as I and II) of Refs. 1 and 2 where the results of the two differed appreciably. Otherwise, density II was used. Transition densities I include the effects of many particle-hole pairs in the final state, but not the effects of ground-state correlations (i.e., $Y_\nu=0$). Transition densities II include the effect of some ground-state correlations ($Y_\nu\neq 0$). The results for single-particle transitions (final state represented by a single particle-hole pair) have been included for comparison. The excitation energies obtained in Refs. 1 and 2 for a given level are in general different for I and II, and typically neither energy agrees with the measured excitation energy. The computed results in Sec. IV are labeled by the energies obtained in Refs. 1 and 2 as well as the experimental energies.

The distorted waves used were generated from optical potentials obtained by extrapolation from potentials given at 180 MeV in a recent analysis.[8] This extrapolation was performed by assuming that the potential strengths varied with energy in the same way as the corresponding portions of the two-nucleon interaction. The geometrical parameters were fixed. The potential for ^{12}C was also used for ^{16}O since the data were not available for the latter nucleus. The optical parameters are listed in Table II. The potentials obtained in this way are not entirely satisfactory and there are uncertainties in the peak inelastic cross sections of the order of 10% for ^{12}C and ^{40}Ca because of this, and perhaps more for ^{16}O.

The results of these calculations are shown in Figs. 1 through 8 along with some of the available experimental data. Polarization results were included only for the two levels of ^{12}C since little or no data currently exist for the other cases. The polarization calculated by Born approximation has been included for transition densities II to illustrate the effects of spin-orbit coupling in the optical potential. (The Born approximation result for the polarization is hardly affected by distorted waves with *no* spin-orbit coupling, cf. Ref. 5.)

IV. LEVELS OF ^{12}C

4.43 MeV: 2^+, $T=0$. The GVM density yields an enhancement of more than three in the peak cross section over the single-particle result. The approximation I density does not provide sufficient enhancement to match the experimental data (see Fig. 1). The degree

TABLE II. Optical potentials used here. These parameters were obtained from the potentials in Ref. 7 by extrapolating the potential strengths as described in Ref. 5 and in the text.

	^{12}C	^{40}Ca
V	22.1	22.0
r	0.902	1.01
a	0.452	0.548
W	15.9	16.6
r'	1.19	1.36
a'	0.556	0.542
V_s	4.31	4.26
W_s	−0.11	−2.14
r_c	1.33	1.32

[6] D. M. Brink and G. R. Satchler, *Angular Momentum* (Oxford University Press, London, 1962).

[7] A. M. Green and A. Kallio (private communication).

[8] G. R. Satchler and R. M. Haybron, Phys. Letters **11**, 313 (1964).

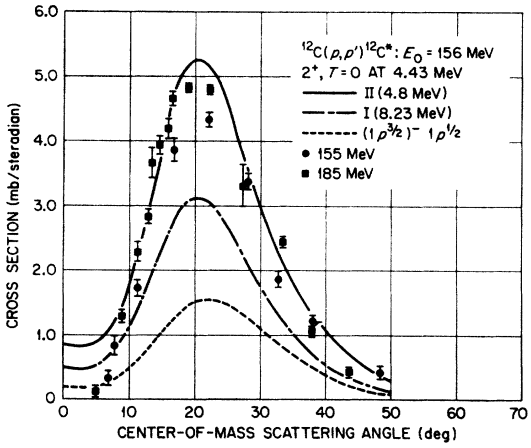

FIG. 1. Cross section for the first excited state of carbon. Shown are the density I, density II, and $1p^{3/2}$ hole$-1p^{1/2}$ particle results for the cross section. Here, and in the following figures we have labeled the results for the two densities with the computed excitation energy. The experimental energy is given after the quantum numbers of the level. The data were taken from Refs. 9 and 10.

of enhancement can be seen to be dependent on scattering angle.

The polarization is substantially altered from the single-particle result in the region of its maximum value and at maximum is close to the extreme L-S coupled result quoted in Ref. 4. The spin-flip parameter $\lambda(\theta)$,[4,5] which measures the ratio of nuclear spin-flip to non-spin-flip matrix elements is small for the GVM density out to large angles as can be seen in Table III. $\lambda=0$ for extreme L-S coupling and 0.75 for j-j coupling (single particle). Note that optical spin-orbit coupling modifies the polarization appreciably and must be included. An attempt to infer λ from polarization data without the spin-orbit contribution would yield erroneous values.

Experimental points obtained at Orsay[9] at 155 MeV and Uppsala[10] at 185 MeV are shown in Fig. 1. The data from these two sources seem in reasonable agreement as to magnitude and shape of the cross section allowing for the difference in bombarding energy. The calculated result for density II shows agreement with the data although the maximum value of the computed cross section is perhaps 10% too large. However, in view of the uncertainty mentioned previously, a different optical potential could remove this discrepancy (or enhance it).

The polarization data in Fig. 2 come from several sources[11]; the latest and most precise data are those of Marty[12] at 155 MeV shown with solid black circles. The computed polarization agrees qualitatively with the data but not in detail. If one attempts to imagine the energy dependence of the first large "loop" of the polarization as indicated by the data at the various energies, it would seem the calculated result for density II is too large below 30° for distorted waves. The plane-wave polarization (which here is essentially the same as distorted waves without spin-orbit coupling) seems to be more consistent with the data. On the other hand, the large negative polarization at 50° which is indicated by Marty's data can only be obtained with the inclusion of spin-orbit distortion.

TABLE III. The spin-flip parameter λ as a function of scattering angle θ. $\lambda=0.75$ for a $1p^{3/2}-1p^{1/2}$ single-particle transition.

θ	0	10	20	30	40	50
λ	0.0280	0.0335	0.0471	0.0725	0.113	0.172

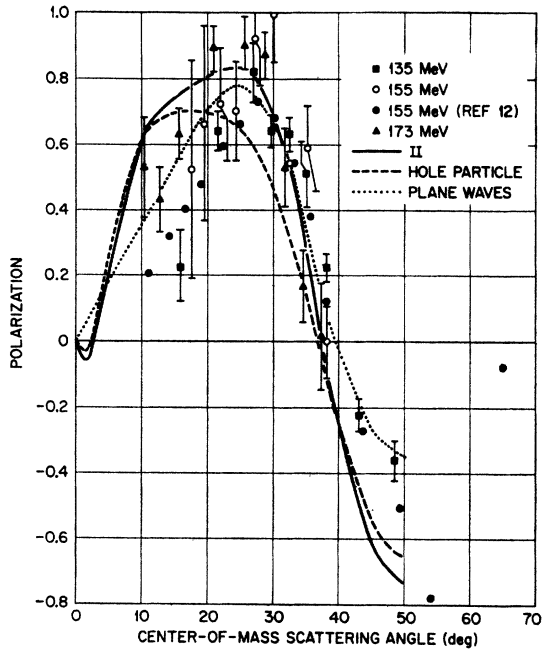

FIG. 2. Polarization for the first level of carbon. The polarization predicted by densities I and II are essentially the same so that only the curve for II has been shown. The key to the curves is the same as in Fig. 1 and will be used through Fig. 8; that is, density II is a solid line, density I is long and short dashes, and the single-particle curve is short dashes. The dotted curve is the plane-wave result for density II. This convention will also be maintained through Fig. 8. The data are described briefly in the text.

9.6 MeV: 3^-, T=0. The approximation II density yields an enhancement of 50% over the single-particle results. Density I does not provide any appreciable enhancement (see Figs. 3 and 4).

The difference in the polarization between II (I provides essentially the same polarization) and the single-particle result is due to the change in λ. The single-particle transition is $p^{3/2}$ to $d^{3/2}$ with $\lambda=0.67$. The GVM transition densities include an admixture of $p^{3/2}-d^{5/2}$ with $\lambda=0.055$ for density II. λ is constant for

[9] J. C. Jacmart, thesis, Paris (unpublished); J. C. Jacmart, J. P. Garron, M. Riou, and C. Ruhla, Phys. Letters 8, 269 (1964).
[10] D. Hasselgren, P. U. Renberg, O. Sundberg, and G. Tibell, Nucl. Phys. (to be published).
[11] P. Hillman, A. Johansson, and H. Tyren, Nucl. Phys. 4, 648 (1957). This reference contains the 173-MeV results and references to other data.
[12] N. Marty (private communication).

both densities since only $1p$-$1d$ transitions are included. The presence of $3\hbar\omega$ particle-hole pairs ($1s$-$1f$, $1p$-$2d$, etc.) could, in principle, be detected from the experimental polarization by the demonstration of an angular variation of λ. This, of course, would rely on an accurate determination of the spin-orbit portion of the optical potential.

The cross-section data in Fig. 3 were taken from Refs. 9 and 10. The data on this level from the two sources seem to be inconsistent. The calculated cross section for density II favors the 155-MeV data but the agreement is not particularly good. Although the magnitude of the peak cross section obtained here agrees with experiment, it occurs at a somewhat larger angle. This is a definite discrepancy; the multipolarity of the transition essentially determines the angle at which the peak cross section occurs, and rather substantial changes in the transition density or the effective interaction are required to shift this angle.

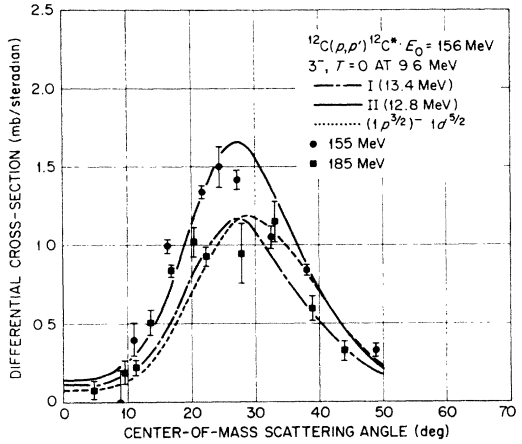

FIG. 3. The cross section for the 9.6-MeV level of carbon is shown here. The apparent structure in the 185-MeV data is unexplained.

The polarization results are shown in Fig. 4. In view of the paucity of data[11] and the large associated errors, we can only claim consistency with experiment.

The II transition density used here was calculated using $1\hbar\omega$ pairs. The discrepancy we have noted between calculation and measurement in Fig. 3 could be due, in whole or in part, to this restriction. As previously mentioned, inclusion of $3\hbar\omega$ pairs would produce an angular variation of λ and this could materially alter the shape of the cross section.

The possibility that the form of the two-nucleon amplitude used is inadequate to the purpose must also be considered. This will be discussed briefly in Sec. VII. However, it should be noted that a similar discrepancy occurs in the comparison between electron scattering data and density II for this level (Ref. 3), so that some or all of the discrepancy must come from the inadequacy of the transition density.

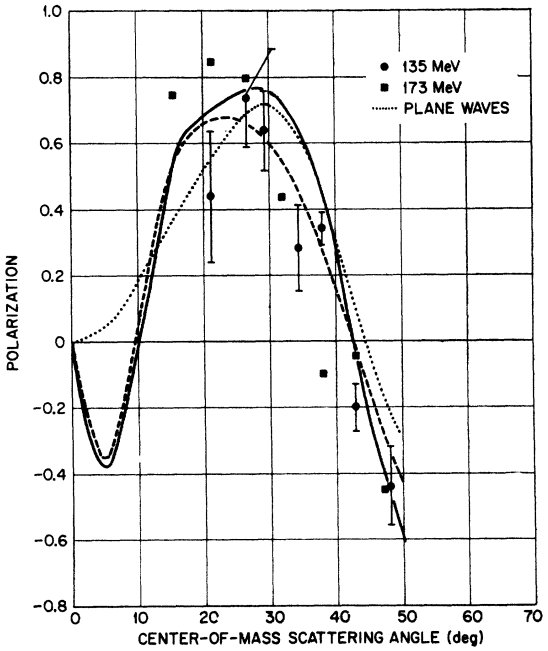

FIG. 4. The polarization for the 9.6-MeV level of ^{12}C.

V. LEVELS OF ^{16}O

6.13 MeV: 3^-, $T=0$. The computed cross section for this level is shown in Fig. 5 together with the Uppsala

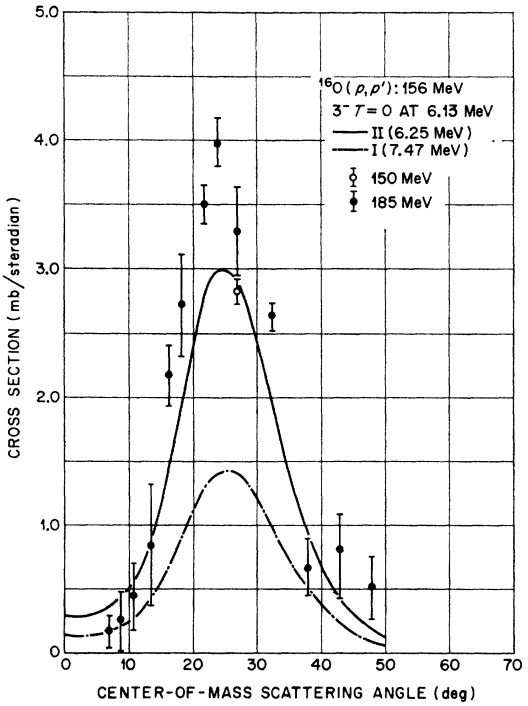

FIG. 5. The cross-section for the 6.13-MeV level of ^{16}O. The discrepancy between the peak experimental cross section and the computed one may be due to the unresolved 0^+ level.

data taken at 185 MeV (Ref. 10). (The calculations throughout have been performed at 155 MeV. The angular location of the peak cross section moves to smaller angles as the bombarding energy is increased and this must be allowed for when comparing the calculations to the data taken at 185 MeV. One does not expect the magnitude of the peak cross section to vary substantially with energy in this range.) Also shown is a single point obtained in a $(p,p'\gamma)$ experiment at 150 MeV.[13]

It can be seen that the approximation II density provides an enhancement which agrees with the single point at 150 MeV. The result is about a millibarn too small compared to the 185-MeV data, but this latter experiment probably did not resolve the 6.05 MeV, 0^+ and 6.13, 3^- levels.[10] If we assume that our result is correct for the 3^- member of this group, then the 0^+ level must be contributing 0.5—1.0 mb/sr at 25°. This is certainly reasonable (and of the order of the measured contribution from the 0^+ level of ^{12}C, which has a comparable monopole moment, given in Ref. 10), although somewhat larger than the value of 0.23±0.14 mb/sr given in Ref. 13. The transition to the 6.05 MeV, 0^+ level is probably explained in terms of 2 particle-2 hole and 4 particle-4 hole contributions as in the calculations being performed by Green *et al.*[14] DWIA calculations using these transition densities may serve to clarify the structure of the 6.13-MeV group. The analysis of electron scattering exciting this level,[15] gives an identical result in that, by comparison with the GVM vector, about 25% of the observed cross section is attributed to the 0^+ level.

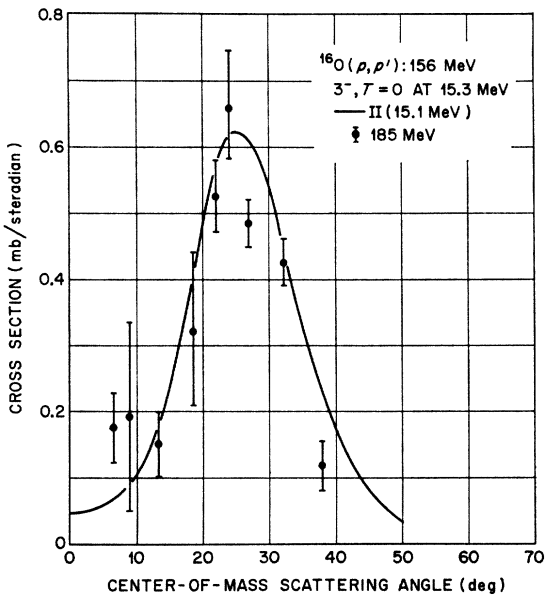

FIG. 6. The 3^- level of ^{16}O at 15.1 MeV given in Ref. 2. This seems to compare reasonably with the 185-MeV data.

15.3 MeV: 3^-, $T=0$. The cross section for the 15.1 MeV, 3^-, $T=0$ level of Ref. 1 is given in Fig. 6 compared to the data obtained in Ref. 10 at 15.3 MeV. The agreement is good and indicates that this experimental group is likely to be predominantly 3^-, $T=0$.

VI. LEVELS OF ^{40}Ca

3.7 MeV: 3^-, $T=0$. The cross section and polarization results for this level are shown in Figs. 7 and 8. Density II was used with two values of the oscillator parameter: $\alpha=0.11$ as used by Gillet and Sanderson and $\alpha=0.132$. The latter value, computed by Swift[16] seems to provide a better approximation to the parabolic Fermi distribution obtained from elastic electron-scattering data[17] than the value used in Ref. 2.

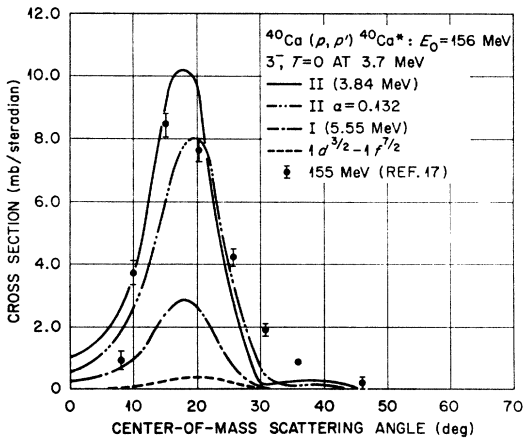

FIG. 7. The 3.7-MeV level of ^{40}Ca is shown here. The reduction in the peak cross section for $\alpha=0.132$ is due to the fact that this oscillator parameter corresponds to a small effective radius. This increases the effects of absorption in addition to displacing the peak to a slightly larger angle.

The approximation I density provides considerable enhancement over the single-particle density, but is lower than the Orsay experiment[18] by a factor of 4. Density II provides considerable enhancement for either value of the oscillator parameter. The cross section computed with $\alpha=0.11$ (the value used in Ref. 2) seems to be in reasonable agreement with experiment. The calculated peak cross section is somewhat too large, but it occurs at the angle required by the data. It should be noted however that no correction has been made for center-of-mass effects, so that the precise

[13] D. J. Rowe, A. B. Clegg, G. L. Salmon, and P. S. Fisher, Proc. Phys. Soc. (London) **80**, 1205 (1962).
[14] G. E. Brown and A. M. Green (to be published); J. Borysocvicz and R. K. Sheline, Phys. Letters **12**, 219 (1964).
[15] G. R. Bishop, C. Betourne, and D. B. Isabelle, Nucl. Phys. **53**, 366 (1964).
[16] Daphne Jackson (private communications).
[17] L. R. B. Elton, R. R. Shaw, and A. Swift, P.L.A. Progress Report, Rutherford High Energy Laboratory, Harwell, 1963 (unpublished).
[18] W. J. Hornyak, J. C. Jacmart, M. Riou, J. P. Garron, C. Ruhula, and M. Liu, J. Phys. Radium **24**, 1052 (1963).

value of the oscillator parameter used is not too important.

The large-angle "fit" to the data is much poorer here than for the two levels of ^{12}C. Even if an improvement of the optical potential and a more refined value of the oscillator parameter served to reduce the calculated peak cross section to better agreement with experiment, it is unlikely that the fit to the large-angle data would be improved.

The polarization results indicate a very strong interference between the contribution due to the two-nucleon interaction and that due to the spin-orbit coupling in the optical potential. This is at first surprising in view of the comparatively small spin-orbit effects for the levels of ^{12}C discussed in Sec. IV. However as we shall see in a later section, the spin-orbit polarization increases substantially with increasing atomic weight so that large contributions are expected for ^{40}Ca.

The result in Fig. 8 must be regarded only as an indication that large spin-orbit effects can be expected in the polarization for medium weight nuclei. The few data available for this level (Ref. 11) do not seem to display the structure indicated in the computed result and the general lack of high-energy inelastic polarization data for nuclei other than carbon gives us no basis to claim that such structure exists without further investigation. It should be noted that the polarization results for single-particle and hole-particle densities are qualitatively similar in that they both display the interference effects and therefore this phenomenon seems not to be characteristic of the nuclear structure involved but rather of the relation of the form of the two-nucleon interaction to that of the distorted waves in spin-space. Investigation of the way in which these two contributions to the inelastic polarization combine may provide information about the spin-dependent part of the distorted waves.

6.8 MeV: 2^+ and 3^-, $T=0$. Several levels of ^{40}Ca have been identified in experiment with 17-MeV protons at Colorado[19] in the energy region around 6.8 MeV. Among them ar a 2^+ level at 6.94 MeV and a 3^- level at 7.1 MeV. These two levels probably dominate the 6.8 MeV group in Ref. 18. Gillet and Sanderson (Ref. 2) predict a 3^-, $T=0$ state at 7.15 MeV which may correspond to the octupole level in question. The calculations of Ref. 2 only include negative particle hole-particle states for ^{40}Ca so that we do not have a DWIA result for the quadrupole level. Therefore we postpone discussion of these levels until Sec. VI where we shall attempt to include the quadrupole level using a collective form factor.

VII. DISCUSSION

We have obtained reasonable agreement with experiment for the levels considered in this section. There is also agreement with experimental electron inelastic scattering for three of the levels. The comparison of the electron and proton inelastic scattering shows that the DWIA is indeed a useful approximation for protons in this energy region, and the two together show that the particle-hole calculations, including ground-state correlations, give a remarkably good description of the transition densities. It would be an achievement to be able to comment further on the validity of the transition densities and hence of the structure calculations which produced them. Unfortunately, we are not as yet in a position to do so.

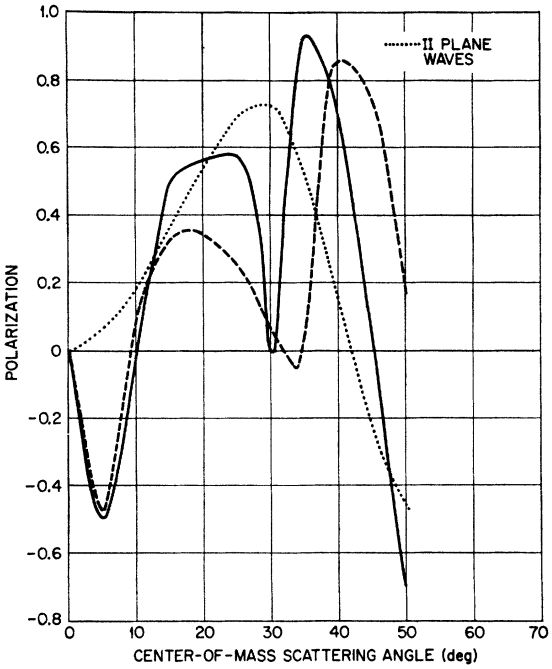

FIG. 8. No polarization data have been included here. Note that the plane-wave polarization for density II is typical of a normal parity, $\Delta T=0$ transition (Ref. 4). However, the spin-orbit coupling seems to have a radical effect on both the single particle (dashed) and density II (solid) prediction. In the presence of such a large effect we do not claim the result in Fig. 8 is accurate without further study, but only that spin-orbit distortions can be quite significant for medium-light nuclei (see Fig. 12) and must be accounted for.

The DWIA calculations use the following components: (1) the transition density for the excitation, (2) distorted waves obtained from an optical potential which fits the elastic data at the same energy, and (3) the two-nucleon transition matrix.

The "effective radius" of the transition density and the multiploarity of the transition essentially determine the location of the peak cross section. The strength and shape of the absorptive part of the optical potential determine the attenuation of the cross section relative to Born approximation.

Distorted waves do not radically affect the shape of the cross section at these energies (except at diffraction minima), but have a major effect on the normalization. The cross-section shape then depends mainly on the

[19] W. S. Gray, R. A. Kenefick, and J. J. Kraushaar, Phys. Rev. (to be published).

transition density and the form of the two-nucleon interaction.

As far as the two-nucleon interaction is concerned, there are several uncertainties, most of which are discussed in Ref. 4. One is the validity of the impulse approximation. Granting this, another uncertainty is the replacement of off-energy-shell by on-energy-shell two-nucleon matrix elements, and the replacement of the resulting nonlocal operator by a local one. There is a further, nonessential, approximation made, also discussed in Ref. 4, of using "asymptotic" kinematics for calculating two-nucleon scattering inside the nucleus. More immediately to the point, the two-nucleon scattering matrix used here was calculated from the Gammel-Thaler phase shifts. Many recent more accurate fits to the two-nucleon data are now obtainable which can differ considerably from the Gammel-Thaler amplitudes, and the calculations are being repeated with these more recent amplitudes to test the sensitivity of the inelastic cross sections to the form of the two-nucleon interaction.

The results of the present calculation show that with transition densities agreeing with electron scattering data and optical-potential obtained from proton elastic scattering, the nucleon-nucleon interaction adopted here is adequate, but the uncertainties mentioned above prevent any quantitative statements about the bearing on transition densities on deviations from experiment. For this reason the transition densities in the present calculation have not been corrected for center-of-mass effects. Actually the comparison of experiment with theory involves only certain portions of the two-nucleon scattering matrix, and this is investigated in the next section.

VIII. TWO-NUCLEON INTERACTION

The two-nucleon interaction used here can be expressed in the form (Ref. 4)

$$t=A+B\boldsymbol{\sigma}_t\cdot\hat{n}\boldsymbol{\sigma}_p\cdot\hat{n}+C(\boldsymbol{\sigma}_t+\boldsymbol{\sigma}_p)\cdot\hat{n}+E\boldsymbol{\sigma}_t\cdot\hat{p}\boldsymbol{\sigma}_p\cdot\hat{p}+F\boldsymbol{\sigma}_t\cdot\hat{q}\boldsymbol{\sigma}_p\cdot\hat{q}, \quad (4)$$

where $\hat{q}$, $\hat{n}$, $\hat{p}$ form a right-handed set of orthogonal unit vectors, $\boldsymbol{\sigma}_t$ and $\boldsymbol{\sigma}_p$ are the spin operators for the target nucleon and projectile, respectively, and the coefficients A, B, C, E, F are functions of incident energy and momentum transfer. These latter quantities are determined to fit free, two-nucleon scattering data and we have used the set obtained from the Gammel-Thaler phase shifts as discussed in Ref. 3.

The portion of (4) which is effective in the transitions we are considering was investigated by performing calculations with the full amplitude, with $B=E=F=0$ and with $B=C=E=F=0$. These calculations were done for the first 2^+ and first 3^- levels of ^{12}C and results are shown in Figs. 9 through 11. The approximation II transition densities were used. The single-particle density was also used for the 2^+ level for comparison.

Inspection of the figures indicates that the two-nucleon amplitude may be well represented, for the transition by

$$t_{\text{eff}}=A+C(\boldsymbol{\sigma}_p+\boldsymbol{\sigma}_t)\cdot\hat{n}. \quad (5)$$

This is a nontrivial result in that it materially reduces the time involved in redoing calculations with various sets of phase shifts. The form in (5) is adequate for these levels because of their small λ values and is anticipated by the plane wave theory of Ref. 4. Note that the scalar portion of the interaction A is dominant only in the forward direction at this energy. At lower energies the spin-orbit portion of the interaction C diminishes in importance relative to the scalar portion so that the angular region over which the effective t is a scalar will increase with decreasing energy.

Calculations similar to those described here were also performed for the 3.7-MeV level of ^{40}Ca and here again, the effective portion of t is that given in (5).

This indicates that at the lower energies, 40 to 70 MeV, the scalar central part of the two-nucleon interaction only will be involved in the excitation of these collective states and that with good transition densities

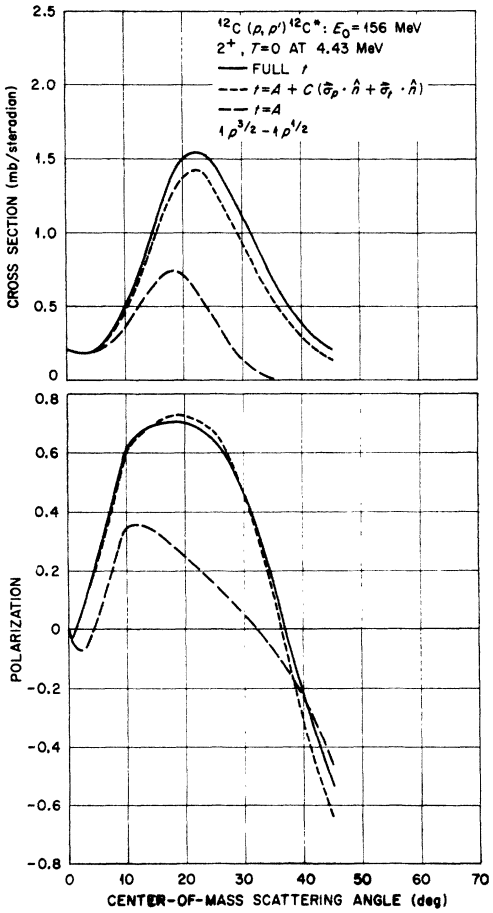

FIG. 9. Here we show the importance of the various portions of the t matrix on the first quadrupole transition in ^{12}C using a single-particle density.

and good elastic-scattering data this part of the effective two-nucleon interaction can be found with good accuracy from inelastic-scattering experiments. Other states, of course, such as the magnetic dipole state in ^{12}C in 15.11 MeV involve different parts of the two-nucleon interaction and this will be investigated in detail elsewhere.

IX. COLLECTIVE FORM FACTORS

The inelastic scattering of medium-energy protons and alpha particles[19,20] has been analyzed with considerable success using a deformed, optical-potential interaction based on the collective theory of nuclei. In such a picture, the incident particle interacts with a nonspherical optical potential. The spherical portion of the potential is the ordinary optical potential which produces elastic scattering. The nonspherical parts produce inelastic transitions between collective vibrational or rotational states (see Ref. 19). The calculation of the inelastic cross section in this model contains only one free parameter for axially symmetric, even-even nuclei called β. This measures either the degree of deformation of the optical well or the mass parameter in

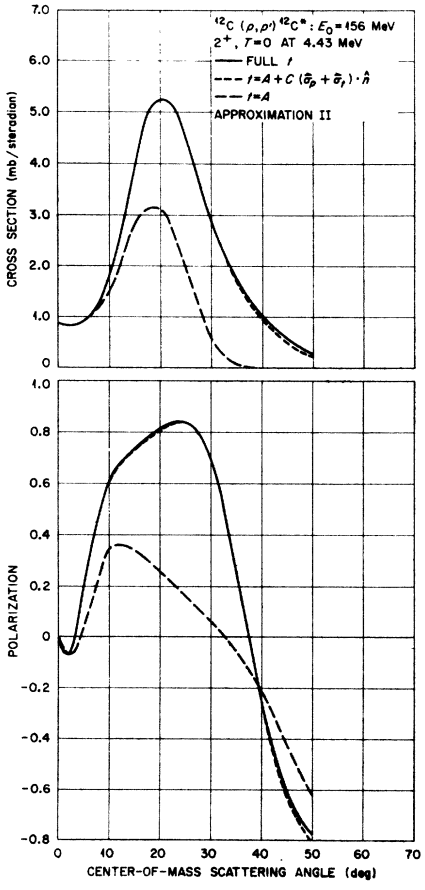

FIG. 10. Density II has been used here to compare with the single-particle results in Fig. 9. Note that the tensor terms are virtually excluded by the form of the transition density.

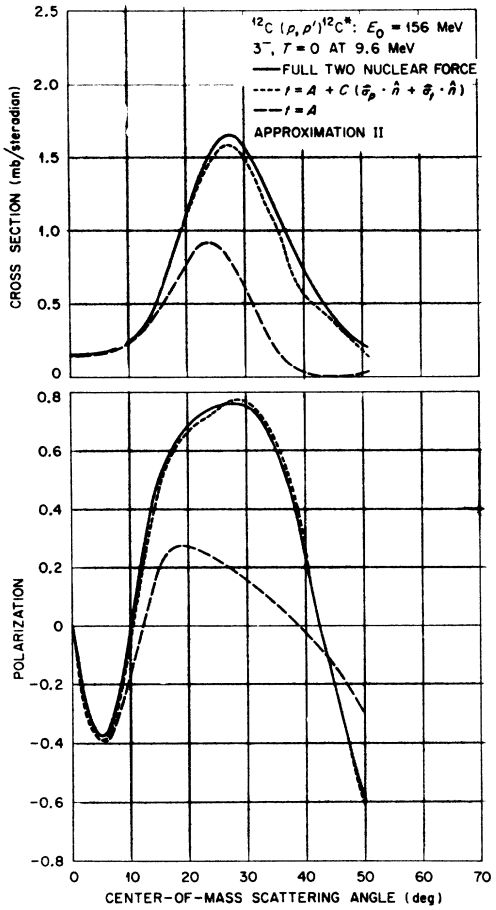

FIG. 11. The importance of the various portions of the t matrix is shown here for the 3^-, 9.6-MeV level of ^{12}C using the approximation II transition density.

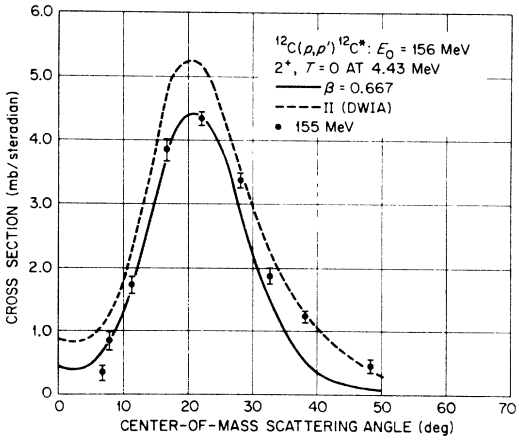

FIG. 12. The collective and DWIA results are compared here with the 155-MeV data. It should be noted that both calculations have a similar angular dependence although the deformation for the collective fit has been chosen to agree with the data.

[20] R. H. Bassel, G. R. Satchler, R. M. Drisko, and E. Rost, Phys. Rev. **128**, 2693 (1962).

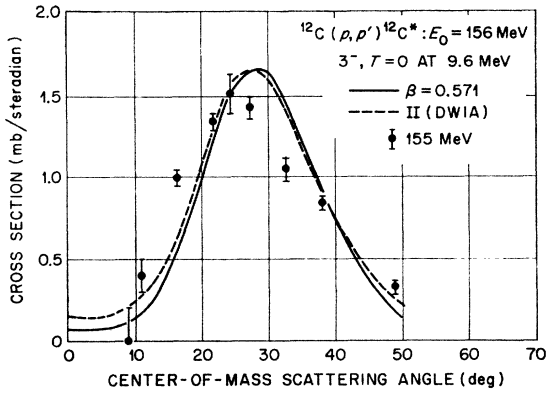

FIG. 13. The two types of calculation agree with each other, but not with the data. The discrepancy between the position of the computed and measured peak cross section indicates that the effective interaction radius is too small.

the vibrational case and is adjusted to fit the inelastic data.

The inelastic cross sections for the 4.43- and 9.6-MeV levels of ^{12}C, the 3.7-MeV level and 6.8-MeV group of ^{40}Ca were calculated using collective form factors and the results are shown in Figs. 12 through 15. The DWIA results for the states of ^{12}C and the 3.7-MeV level of ^{40}Ca obtained in Sec. VIII are included for comparison. The DWIA result for the 7.15 MeV, 3^- level of Ref. 2 is shown in Fig. 15.

The form factors used here are complex: they are related to the derivative of the optical potential excluding the spin-orbit term. In a recent analysis of the inelastic scattering of 40-MeV protons by several nuclei, Fricke and Satchler[21] expressed some preference for complex coupling as compared to deforming only the real part of the potential. In calculations currently being performed[22] it has been found that the complex coupling is clearly required for 155-MeV protons; in particular,

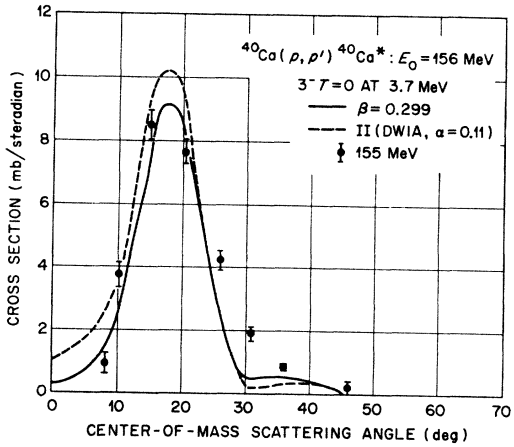

FIG. 14. The value of β used here may be too small by a few percent for a "best" fit.

real coupling for this energy produces inelastic cross sections which consistently peak at too large an angle and in addition yields deformations which are considerably larger than those obtained by other means.

The optical potentials used here and elsewhere in this communication are volume absorbing. The use of surface absorption is being investigated although the results in Ref. 8 indicate some preference for volume absorption at proton energies in this range. It is possible that analysis of the high-energy inelastic data will help to choose between volume and surface absorption, although there is no clear indication of preference at 40 MeV (Ref. 21).

The lower energy proton analyses provide us with values of the deformation of ^{12}C (Ref. 21) and ^{40}Ca.[23] These are displayed in Table IV together with the results obtained here.

The agreement obtained between the collective form factors and the DWIA form factors is surprisingly good, indicating a more than casual connection between the two radically different ways of obtaining the cross sections which must be investigated.

Qualitatively, this result can be understood. The optical potential can always be represented by the expectation value in the ground state of the nucleus of an operator t' which is complex, i.e., ignoring spins and phase-space factors $U_{\rm opt}(r)=\int t'(\mathbf{r}-\mathbf{r}')\rho(\mathbf{r}')d\mathbf{r}'$, where $\rho(\mathbf{r}')$ is the nucleon density in the ground state. This is real, but $U_{\rm opt}$ is complex as $t'(r)$ is complex. At high energies the operator t' is approximately the free nucleon-nucleon scattering operator; at lower energies it is expressible in a power series in this operator. If, for the inelastic scattering, we use the free nucleon-nucleon amplitude t, then the effective transition density $U_{n0}(r)$ causing the transition is found by combining the nucleon-nucleon scattering operator and the transition densities $F^{lS,J}(r)$, $U_{n0}=\int t(\mathbf{r}-\mathbf{r}')F^{lS,J}(r')d\mathbf{r}'$. Now the scattering amplitude is complex and so will give rise to a complex effective transition density similar to the derivative of the optical potential, particularly as $t'\sim t$ at these energies and the nuclear inelastic form factor $F^{lS,J}(r)$ is more peaked relative to the nuclear surface than the ground-state density $\rho(r)$. This con-

TABLE IV. The deformations labeled "low energy" were obtained with 40-MeV protons for ^{12}C and 55-MeV protons for ^{40}Ca. The deformations obtained at 55 MeV for the 6.8-MeV group of ^{40}Ca were not searched on for the best set of values. We have increased β for the 3^- level by 10% to improve our fit.

Level	β(155 MeV)	β(low energy)
$^{12}C2^+$(4.43 MeV)	0.667	0.60 (Ref. 20)
3^-(9.6 MeV)	0.571	0.44 (Ref. 20)
$^{40}Ca3^-$(3.7 MeV)	0.299	0.33 (Ref. 22)
2^+(6.8 MeV)	0.10	0.10 (Ref. 22)
3^-(6.8 MeV)	0.11	0.10 (Ref. 22)

[21] M. P. Fricke and G. R. Satchler, Phys. Rev. **139**, B567 (1965).
[22] R. M. Haybron (to be published).
[23] K. Yagi, H. Ejiri, M. Furukawa, Y. Ishizaki, M. Koike, K. Matsuda, Y. Nakajima, I. Nonaka, Y. Saji, E. Tanaka, and G. R. Satchler, Phys. Letters **10**, 186 (1964).

nection has been mentioned before, particularly by Jackson,[24] in connection with the inelastic scattering of alpha particles. For this case, however, only the real part of the optical potential and its derivative have to be taken into account. In the present case, there are two important differences. The first is that the imaginary part of the optical potential is extremely important. This has a larger radius than the real part so that taking the derivative of the real part only as the effective transition density in the macroscopic model gives a form which has too small a radial extension and gives an inelastic cross section peaking at too large a momentum transfer. Also, because of the nucleon spin, two components of the effective interaction [Eq. (5)] are important in the microscopic model. Near the cross-section peak and beyond, the spin-dependent part of the effective interaction is extremely important (see Figs. 10 and 11) so that the correct position of the cross-section peak is given by a combination of the microscopic form factors and the spin-dependent and spin-independent parts of the effective interaction acting incoherently. It is the spin-dependent part of the effective interaction which gives rise to the spin-orbit part of the optical potential. However, this part of the optical potential has been ignored in the collective model and the correct position of the peak cross section has been achieved by means of the large radius for the imaginary part found from the analysis of elastic scattering.

The collective form factors do not reproduce the inelastic polarization. Since they are spin-independent, only the spin-dependent distortion effects in the initial and final channels can produce spin flip and the resulting polarizations do not bear any resemblance to experiment. The polarizations produced for $l=3$ transitions using complex collective form factors for ^{12}C, ^{40}Ca, and ^{56}Fe are shown in Fig. 16. It is noticeable from these curves that the optical-potential spin-orbit-produced polarization increases with A.

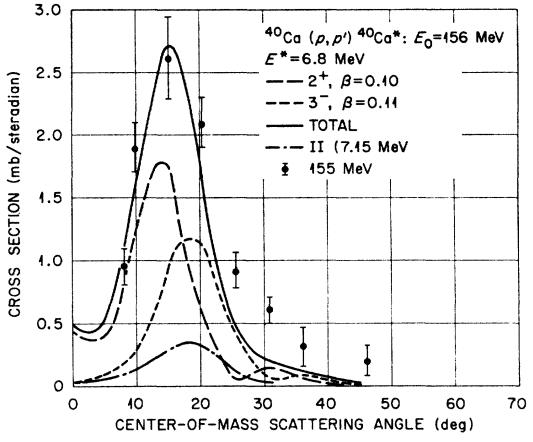

FIG. 15. The curve labeled "total" is the sum of the 2^+ and 3^- collective form-factor cross sections. The DWIA curve found using the 7.15 MeV, 3^- level of Ref. 2 is shown for comparison. Although the fit achieved here with the collective form factors is not particularly good, it would seem that the 7.15 MeV of Ref. 2 does not after all correspond to the 3^- contribution to this experimental group. This of course is supposing that no other strongly excited levels are contained in the data.

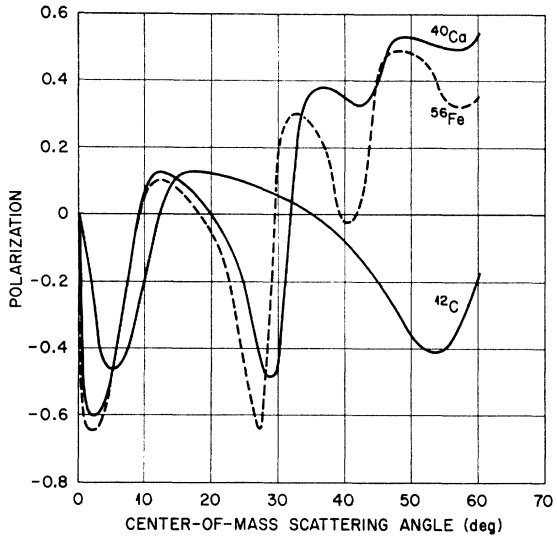

FIG. 16. These polarization were obtained using collective spin-spin-independent form factors. The result for ^{40}Ca shows clearly the source of the strong interference noted in Fig. 8.

For a more valid comparison and investigation in detail of the relation between the macroscopic and microscopic models, the derivative of the optical potential including the spin-orbit term must be used and this is being investigated.

Note: The discrepancy noted between the calculated polarization for the 4.43-MeV level of ^{12}C and the data from Ref. 12 have been pointed out by Perrain and Vinh-Mau[25] recently. Their calculation was done using plane waves, but as we have pointed out, inclusion of spin-orbit distortions serves only to worsen the situation at small angles.

ACKNOWLEDGMENTS

The authors are grateful to N. Marty and G. Tibell for providing them with experimental results prior to publication. They also acknowledge the assistance of V. Gillet, G. E. Brown, A. Kallio, and A. M. Green in elucidating the phases of the vectors used, and of G. R. Satchler for information on the collective model. One of them (RMH) wishes to express his thanks to the staff of Oak Ridge National Laboratory for its aid in this investigation, and the other (HMcM) wishes to thank the Guggenheim Foundation for its assistance, and NORDITA, where part of this work was done, for its hospitality during 1963–4. We especially wish to acknowledge the aid of R. M. Drisko in helping to prepare the code used in these calculations.

[24] D. F. Jackson, Phys. Letters **14**, 118 (1965); N. K. Glendenning and M. Veneroni, Phys. Letters **14**, 228 (1965).

[25] M. Perrain and N. Vinh-Mau, Phys. Letters **14**, 236 (1965).